Dependence of Radiation Dose on Area and Volumetric Mammographic Breast Density Estimation

H. Jing, B. Keller, J.Y. Choi, R. Crescenzi, E. Conant, A. Maidment, D. Kontos
Department of Radiology, Perelman School of Medicine at the University of Pennsylvania
3600 Market St. Suite 360, Philadelphia, PA, 19104

ABSTRACT

Mammographic breast density is a strong risk factor for breast cancer. Studies on imaging dose in mammography have primarily focused on imaging quality and diagnostic accuracy, while little work has been done on understanding its effect on the estimation of breast density. Studies on the effect of dose on mammographic density estimation can be useful in dose reduction for the purpose of density estimation and monitoring. In this study, we investigate the dependence of percent area (PD%) and volumetric (VD%) breast density estimation on imaging dose using an anthropomorphic breast phantom (Rachel, Gammex). A set of digital mammograms were obtained with a GE Senographe 2000D FFDM system, using 220 unique combinations of different imaging physics, namely target/filter, kVp and mAs. Specifically, 8 different mAs settings were defined as corresponding to 10%, 20%, 40%, 70%, 100%, 150%, 200% and 300% of 1.8 mGy reference average glandular dose (AGD) for standard phototimed exposure. Breast density was estimated using fully-automated FDA-cleared software (Quantra v.2.0, Hologic Inc.). The obtained estimates were analyzed to study the effect of the imaging dose, using ANOVA and linear regression. Results show that there is a statistically significant dependence of density estimation on x-ray imaging dose (p-value=0.014 and <0.001 for PD% and VD%, respectively), while the actual variation of the estimation across the different levels of dose is relatively low (standard deviation of 2.87% and 0.66% for PD% and VD% respectively), the differences could be significant when breast density measures are used for risk estimation.

Keywords: Digital Mammography, mammographic density estimation, imaging radiation dose.

1. INTRODUCTION

Mammographic density refers to regions of brightness in the x-ray image associated with fibroglandular tissue, and is a strong independent risk factor for breast cancer (1, 2). For the purpose of screening and diagnosis, breast density is also correlated with the difficulty of detecting cancers in mammography due to the fact that cancer lesions may be masked by dense tissues (2). Significant work has been done in recent years estimating mammographic density has been conducted in recent years (3-5), and its correlation with the risk for breast cancer (6-9). Therefore, understanding the impact of varying radiation doses used in acquire mammographic images on the resultant estimatation of breast density is essential.

Due to the potential harm to patients undergoing breast cancer screening with mammography, the issue of radiation is a major concern in the design and evaluation of mammography systems. Studies related to dose in mammography have primarily focused on image quality and diagnostic accuracy of radiologists. Samei et al. studied the relationship between radiation dose and observer accuracy in the detection of simulated lesions for digital mammography (10), concluding that dose reduction has modest effect on diagnostic accuracy. Huda et al. studied the effect of x-ray tube voltage (kVp) and exposure time (mAs), two important parameters related to exposure, on image quality characteristics (11). It has also been shown that characteristics of image contrast, digital signal intensity, and image contrast to noise ratio (CNR) can be modified by imaging physics including imaging dose (mAs) (11). Desponds developed a computer simulation to study the effect of anode/filter materials on image quality and dose, and it was found that tungsten anode with a rhodium filter allowed a dose reduction without a significant degradation of image quality (12). In a study comparing the image quality using different target/filter materials, it was concluded units with tungsten anodes achieved the lowest patient doses (13).

Similar to the efforts to reduce the radiation dose while maintaining image quality in mammography systems, it is of interest to study whether meaningful and robust estimation of breast density can be obtained at lower radiation dose levels. This would be useful for reducing the radiation dose to women, for example when monitoring changes in

Medical Imaging 2013: Physics of Medical Imaging, edited by Robert M. Nishikawa, Bruce R. Whiting, Christoph Hoeschen,
Proc. of SPIE Vol. 8668, 866827 · © 2013 SPIE · CCC code: 1605-7422/13/$18 · doi: 10.1117/12.2007989

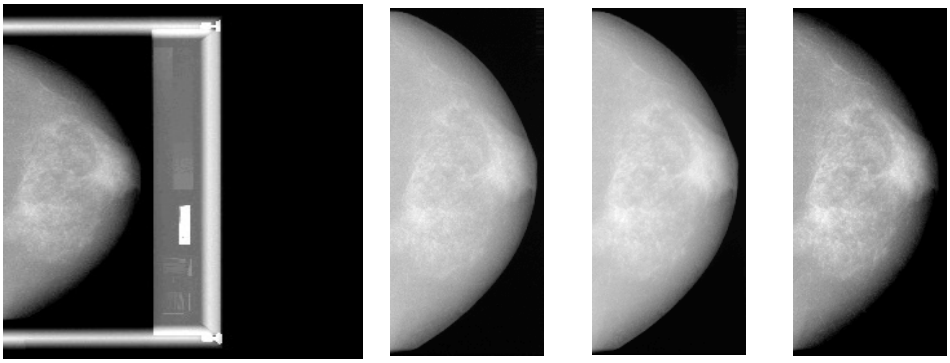

(a) (b) (c) (d)

Figure 1. The original digital mammogram of the Rachel breast phantom (a), and sample mammograms obtained with different dose levels of (b) 10%, (c) 100%, and (d) 300% of the reference AGD. Target/filter is Rh/Rh at 28 kV.

breast density as response to chemoprevention or acquiring baseline density measures for subsequently triaging women to the most appropriate modality for screening (e.g., planar mammography versus whole-breast ultrasound and/or tomosynthesis). Although the effect of the imaging dose on image quality has been extensively studied in the literature, to our knowledge, there is limited work on investigating the effects of varying doses on the estimation of mammographic density, which is a strong risk factor for breast cancer. This could be particularly useful for women at high risk of breast cancer for whom excessive or frequent mammographic screening would be inappropriate.

In this work, we investigate the dependence of area and volumetric breast density estimation on the radiation dose used for digital mammography imaging, using an anthropomorphic breast phantom. Breast phantoms have been used in many imaging studies, especially where multiple exposures may be required (14-16). With the same breast phantom, multiple images are obtained using different settings of target/filter material, kVp and mAs. Subsequently, mammographic densities are estimated using an FDA cleared computational tool, which can provide objective and consistent density estimation results, compared with human readers who typically suffer from inter- and intra- reader variation (3-4). Quantitative analysis using ANOVA and logistic regression is conducted to investigate the dependency of density estimation on imaging physics and whether any such dependency is statistically significant.

2. MATERIALS AND METHODS

An anthropomorphic breast phantom ("Rachel", Model 169, Gammex RMI, Madison, WI) was used in our experiments. This phantom was designed for the evaluation of imaging systems (17), based on a mammogram of a real patient (18). The phantom's original design was based on a composite of two layers of numerically milled Lucite, aligned over a digital printed mercury-enhanced film. The commercial version of the phantom is made from a numerically milled negative mold injected with BR-12 breast tissue equivalent plastic, aligned over a mercury-enhanced film. The low-frequency information of large tissue structures is simulated by the shaped plastic, while high-frequency information is contained in the film. In addition to the simulated breast, a grayscale stepwedge and resolution line pairs are included with the phantom. The simulated breast is primarily fatty with scattered fibroglandular tissue (18). A sample mammogram of this breast phantom is shown in Figure 1(a).

Images were acquired with a full-field digital mammography (FFDM) system (Senographe 2000D, General Electric Health Care, Chalfont St. Giles, UK), compliant with MQSA. Images were acquired in 220 unique combinations of exposure settings. A range of possible combinations of target/filter materials (Rh/Rh, Mo/Rh, Mo/Mo), kV (25-34 kV), and mAs settings were tested. For each target/filter and kV combination, a reference mAs was determined as the setting required to yield an average glandular dose (AGD) of 1.8 mGy for a standard phototimed exposure. Eight mAs settings were then defined relative to the reference mAs: 10%, 20%, 40%, 70%, 100%, 150%, 200%, and 300%. Images were acquired consistently from low to high mAs, in order to reduce the presence of residual signal intensity from previous acquisitions. The system limits the use of Mo filter to a maximum of 32 kV. Rh/Rh at 25 kV, 26 kV, and 27 kV were limited to a maximum of 150%, 200%, and 200% of the reference mAs, respectively, due to anode heating restrictions. The phantom was centered at a constant distance from the chest wall edge of the detector. Two images were acquired with each unique exposure combination, yielding a total of 440 images. Three representative mammograms obtained with kV=28 and different dose levels (mAs) values are shown in Figure 1(b)-(d). For illustration purposes, the mammograms are cropped to highlight the main breast tissue region.

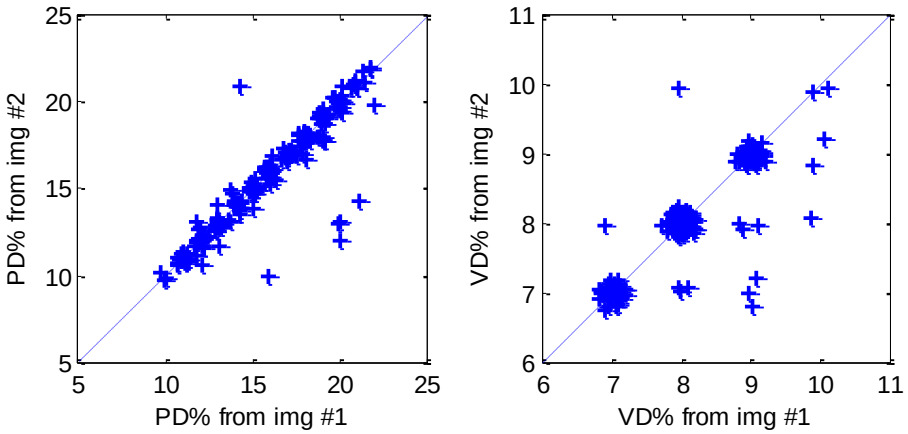

Figure 2. Scatter plot of density estimation results from each two images obtained with same imaging techniques: PD% (Left) and VD% (Right), essentially illustrating the dependence of density estimation on imaging noise.

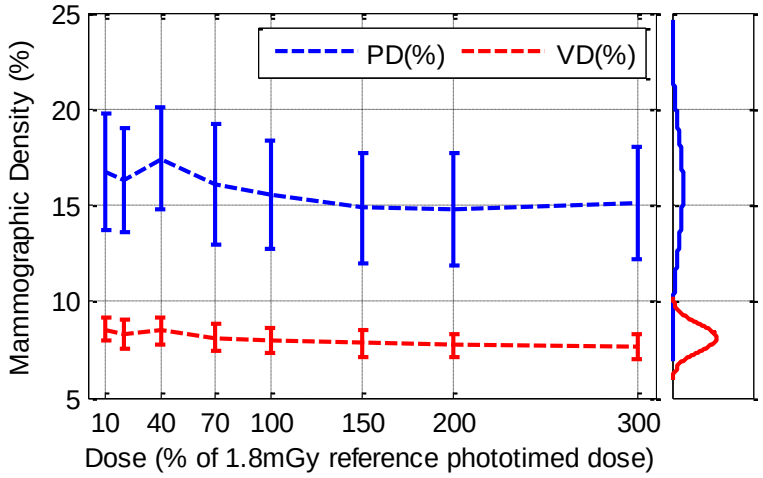

Figure 3. Effect of dose on estimation of PD% and VD%. The estimated densities are fitted with Gaussian distributions and the corresponding probability distribution functions (PDFs) are shown on the right.

For density estimations, a fully-automated and FDA-cleared software was used for percent area (PD%) and volumetric (VD%) breast density estimation (Quantra™ v2.0, Hologic Inc.). The algorithm is based on the widely validated Highnam & Brady method (20), adapted for digital mammography (21). Briefly, the software estimates the thickness of the fibroglandular tissue above each pixel in the image to compute the total volume of fibroglandular tissue in the breast, yielding the estimation of volumetric percentage (21). The estimation is derived based on physical parameters for the breast and the imaging system, and imaging physics of individual exposures, such as the attenuation coefficients for breast tissue, the x-ray spectra for the target material, kVp, mAs and breast thickness. Compared with human readers who typically suffer from inter- and intra- reader variability in density assessment, such automated computational algorithms can be beneficial for generating breast density estimation results in an objective and consistent way. To avoid potential interference to density estimation, the area of the phantom container box in the image was filled with Gaussian noise with statistics same as that of the background, prior to the analysis of a given image.

Statistics for the difference in density estimation for each two images obtained with same imaging settings were summarized to investigate whether density estimation is sensitive to imaging noise. The average of the estimated density for the two images with the same imaging physics was then used for further analysis on the effect of imaging dose on density estimation. To study the variation of the density estimation across different imaging dose, analysis of variance (ANOVA) was performed, to test if the dependence of density estimation is significant, with a p-value threshold of 0.05. Univariate linear regression was also applied to study the linearity of the dependence of density estimation on imaging dose.

3. RESULTS

Percent area (PD%) and volumetric (VD%) breast density were estimated from all 440 phantom images, two for each of the 220 different exposure settings. Figure 2 shows scatter plot of the estimated densities from each two images with same imaging settings. The difference of the density estimation for each of the two images obtained with same imaging setting is calculated. For PD%, the mean and standard deviation of this estimated difference is 0.19% and 1.23% respectively, while for VD%, the mean and standard deviation of this estimated difference is 0.06% and 0.37% respectively. The estimated densities for the two images with same settings were averaged for further analysis. Among all the 220 imaging settings, the mean/standard deviation of the estimated PD% and VD% are 15.79%/2.96%, and 8.08%/0.72%, respectively.

Figure 3 shows the trend of the estimation result when the dose was varied, and for each specific dose, the error bars represent the standard deviation of the estimation when the kV and target/filter material were varied, for all three target/filter material settings. For the reference 1.8 mGy dose, the average (±std) of the estimated phantom PD% is15.528%±2.81% and VD% is 8.02%±0.65%, across the different settings of kVp and target/filter materials. Across all the dose settings, the overall average PD% and VD% are 15.85% and 8.09% respectively. The average of the standard deviations of PD% estimation is 2.87%, and for VD% the average standard deviation is 0.66%. The histograms on the right show the PDFs (probability distribution density) of Gaussian distributions fitted to the estimated densities. The ANOVA yielded p-values of 0.014 and <0.001 for PD% and VD% respectively, which indicates that there is statistically significant dependence of density estimation (for both PD% and VD%) on dose.

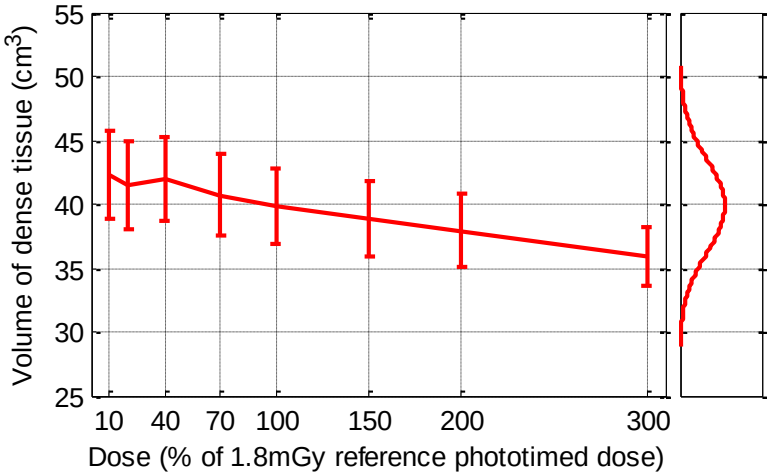

(a)

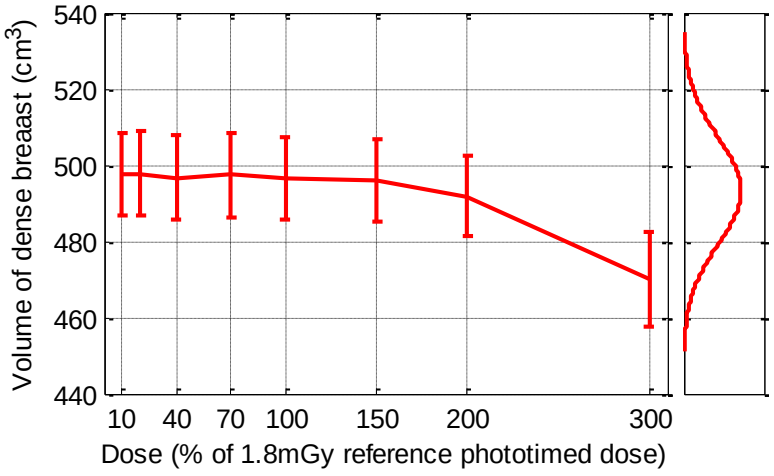

(b)

Figure 4. Effect of dose on estimation of VFG (a) and VB (b). The estimated volumes are fitted with Gaussian distributions and the corresponding probability distribution functions (PDFs) are shown on the right of each plot.

For PD%, the linear regression yielded a p-value=0.001 with slope coefficient of -0.72, and R^2=0.051. For VD%, the linear regression yielded a p-value<0.001 with slope coefficient of -0.31, and R^2=0.15. Further, the estimation results of the absolute volume of fibroglandular (e.g., dense) tissue and the volume of the breast (with respect to the radiation dose) are shown in Figure 4(a) and (b), respectively.

4. DISCUSSION

Our results suggest that digital mammography breast density estimation is statistically significantly dependent on radiation dose. However, the actual magnitude of variation of the estimated density is relatively low, compared to the standard categories [e.g., BIRADs or Boyd scale (1)] that are commonly considered in clinical practice. Therefore, lower doses could be potentially acceptable for the purpose of density assessment and monitoring, for example to determine density changes during and after chemoprevention interventions for high-risk women or when baseline density measures are needed to triaging women with dense breast to the most appropriate modality for screening (e.g., digital mammography versus whole-breast ultrasound and/or tomosynthesis).

The results from linear regression show an interesting trend for the density estimation when the radiation dose is varied. Specifically, the coefficients from the linear regression are all negative, which means that the estimation for both the absolute and density measurements decrease when the radiation dose increases. This may be attributed to the fact that a higher dose will result in more tissue penetration with the resultant digital mammographic image saturated, particularly in the peripheral region of the breast area, as shown in Figure 1(d). This effect may bias the estimation algorithm which will tend to treat the overpenetrated peripheral fibroglandular tissues as fat rather than density, causing the estimation of VFG, PD% and VD% to be lower with higher levels of radiation dose, as shown in Figure 3 and Figure 4. Similarly, the over saturation due to high radiation dose may also lead to under-estimation of the breast volume, which can be seen from Figure 1(d) as well.

By comparing the plots for VB and VFG in Figure 4, it is interesting to note that their estimations are moderately correlated. An average correlation coefficient of 0.58 was obtained on the estimated VB and VFG for all imaging settings. This might also explain the relatively small variation of the estimated volumetric density as shown in Figure 3, which is calculated as the ratio of the volume of dense tissue to the whole breast. It is observed that with radiation dose higher than 100% of AGD, the drop of VFG and VB estimation is quite clear, while the estimated density tends to remain stable. This observation suggests that the density estimation is less affected by varying radiation dose, due to the fact that the radiation dose has similar or correlated effects on VFG and VB.

Our conclusions may be limited in the following aspects. First, only a phantom breast with low breast density was used in this work. This is because it would be challenging to perform similar analysis with real clinical exposures and data, as such an approach may not be appropriate for this kind of sequential imaging studies where multiple imaging exposures are required and could cause excessive radiation, inappropriate for imaging women. Also, it would be more reasonable to experiment with breast phantoms at different levels of density instead of one phantom with low density. This may be an extension of this work when more suitable imaging phantoms are available. Further, only one density estimation tool was used. Future work could also include the evaluation of additional density estimation algorithms in this setting, and it allows more systematic investigation for the relative robustness (of density estimation results) against imaging physics and radiation dose.

5. CONCLUSION

We investigated the dependency of density estimation on x-ray imaging dose, using an anthropomorphic breast phantom, and FDA-cleared software. It was found that the variations in the estimation of density are limited in terms of clinically used categories of breast density [BIRADs and Boyd categories (1)], even though the dependence of density estimation on imaging physics is statistically significant. The relatively small variation of density estimation with respect to imaging dose suggests that mammography performed at doses lower than AGD may be feasible for breast density assessment monitoring or for triaging patients by density for various screening modalities. These results are encouraging, particularly considering that for the purpose of our experiments, both the phantom and the density estimation software were used outside of their originally intended dose limits and image acquisition settings, showing relative robustness. Further investigation is currently underway, to also determine the effects of kV and target/filter combination, also considering the potential limitations of the specific phantom design in terms of energy dependence.

ACKNOWLEDGEMENT

This work was supported in part by the American Cancer Society (ACS) Research Scholar Grant (RSGHP-10-108-01-CPHPS), the National Institutes of Health/National Cancer Institute Research Grants (1U54CA163313-01, R01-CA161749-01A1) and by a Breast Cancer Alliance Young Investigator Research Grant.

REFERENCES

1. Boyd NF, Guo H, Martin LJ, Sun L, Stone J, Fishell E, Jong RA, Hislop G, Chiarelli A, Minkin S, Yaffe MJ. Mammographic density and the risk and detection of breast cancer. New England Journal of Medicine. 2007;356(3):227-36.
2. Yaffe MJ. Mammographic density. Measurement of mammographic density. Breast Cancer Research. 2008;10(3):209.
3. Karssemeijer N. Automated classification of parenchymal patterns in mammograms. Phys Med Biol. 1998;43(2):365-78.
4. Tagliafico A, Tagliafico G, Tosto S, Chiesa F, Martinoli C, Derchi LE, Calabrese M. Mammographic density estimation: comparison among BI-RADS categories, a semi-automated software and a fully automated one. Breast. 2009;18(1):35-40.
5. Castella C, Kinkel K, Eckstein MP, Sottas PE, Verdun FR, Bochud FO. Semiautomatic mammographic parenchymal patterns classification using multiple statistical features. Acad radiology. 2007;14(12):1486-99.
6. Palomares MR, Machia JRB, Lehman CD, Daling JR, McTiernan A. Mammographic density correlation with gail model breast cancer risk estimates and component risk factors. Cancer Epid. Biomar. 2006;15(7):1324-30.
7. Li H, Giger ML, Huo Z, Olopade OI, Lan L, Weber BL, Bonta I. Computerized analysis of mammographic parenchymal patterns for assessing breast cancer risk: effect of ROI size and location. Med Phys. 2004;31(3):549-55.
8. Harrison DA, Duffy SW, Sala E, Warren RM, Couto E, Day NE. Deterministic models for breast cancer progression: application to the association between mammographic parenchymal pattern and histologic grade of breast cancers. Journal of clinical epidemiology. 2002;55(11):1113-8.
9. Wei J, Chan HP, Wu YT, Zhou C, Helvie MA, Tsodikov A, Hadjiiski LM, Sahiner B. Association of computerized mammographic parenchymal pattern measure with breast cancer risk: a pilot case-control study. Radiology. 2011;260(1):42-9. PMCID: 3135878.
10. Samei E, Saunders RS, Jr., Baker JA, Delong DM. Digital mammography: effects of reduced radiation dose on diagnostic performance. Radiology. 2007;243(2):396-404.
11. Huda W, Sajewicz AM, Ogden KM, Dance DR. Experimental investigation of the dose and image quality characteristics of a digital mammography imaging system. Medical physics. 2003;30(3):442-8.
12. Desponds L, Depeursinge C, Grecescu M, Hessler C, Samiri A, Valley JF. Influence of anode and filter material on image quality and glandular dose for screen-film mammography. Phys Med Biol. 1991;36(9):1165-82.
13. Emanuelli S, Rizzi E, Amerio S, Fasano C, Cesarani F. Dosimetric and image quality comparison of two digital mammography units with different target/filter combinations: Mo/Mo, Mo/Rh, W/Rh, W/Ag. La Radiologia medica. 2011;116(2):310-8.
14. Liu X, Lai CJ, Whitman GJ, Geiser WR, Shen Y, Yi Y, Shaw CC. Effects of exposure equalization on image signal-to-noise ratios in digital mammography: a simulation study with an anthropomorphic breast phantom. Medical physics. 2011;38(12):6489-501. PMCID: 3247925.
15. Assiamah M, Nam TL, Keddy RJ. Comparison of mammography radiation dose values obtained from direct incident air kerma measurements with values from measured X-ray spectral data. Applied radiation and isotopes :including data, instrumentation and methods for use in agriculture, industry and medicine. 2005;62(4):551-60.
16. Molloi S, Xu T, Ducote J, Iribarren C. Quantification of breast arterial calcification using full field digital mammography. Medical physics. 2008;35(4):1428-39.
17. Caldwell CB, Yaffe MJ. Development of an anthropomorphic breast phantom. Medical Physics. 1990;17(2):273-80.
18. Caldwell CB, Fishell EK, Jong RA, Weiser WJ, Yaffe MJ. Evaluation of mammographic image quality: pilot study comparing five methods. AJR American Journal of Roentgenology. 1992;159(2):295-301.
19. Agner SC, Xu J, Fatakdawala H, Ganesan S, Madabhushi A, Englander S, Rosen M, Thomas K, Schnall M, Feldman M, Tomaszewski J, editors. Segmentation and classification of triple negative breast cancers using DCE-MRI. 2009 IEEE International Symposium on Biomedical Imaging: From Nano to Macro (ISBI 2009); 2009 2009. p. 1227-30.

20. Highnam R, Jeffreys M, McCormack V, Warren R, Davey Smith G, Brady M. Comparing measurements of breast density. Phys Med Biol. 2007;52(19):5881-95.
21. Hartman K, Highnam R, Warren R, Jackson V, editors. Volumetric Assessment of Breast Tissue Composition from FFDM Images. Digital Mammography (IWDM); 2008: Springer-Verlag Berlin Heidelberg; 2008. p. 33-9.